Letter

Spectra of near-equilibrium adverse-pressure-gradient turbulent boundary layers

Ramón Pozuelo, Qiang Li, Philipp Schlatter, and Ricardo Vinuesa
FLOW, Engineering Mechanics, KTH Royal Institute of Technology, SE-100 44 Stockholm, Sweden

(Received 21 July 2022; accepted 20 January 2023; published 22 February 2023)

With the availability of new high-Reynolds-number (*Re*) databases of turbulent boundary layers (TBLs) it has been possible to identify in detail certain regions of the boundary layer with more complex behavior. In this study we consider a unique database at moderately-high *Re*, with a nearconstant adverse pressure gradient (APG) [Pozuelo *et al.*, J. Fluid Mech. **939**, A34 (2022)], and perform spectral analysis of the Reynolds stresses, focusing on the streamwise component. We assess different regions of the APG TBL, comparing this case with the zero-pressure-gradient (ZPG) TBL, and identify the relevant scaling parameters as well as the contribution of the scales of different sizes. The small scales in the near-wall region up to the near-wall spectral peak have been found to scale using viscous units. In APG TBLs, the largest scales close to the wall have a better scaling with the boundary-layer thickness (δ_{99}), and they are significantly affected by the APG. In the overlap and wake regions of the boundary layer, the small energetic scales exhibit a good scaling with the displacement thickness (δ^*) while the larger scales and the outer spectral peak are better scaled with the boundary-layer thickness. Also, note that the wall-normal location of the spectral outer peak scales with the displacement thickness rather than the boundary layer thickness. The various scalings exhibited by the spectra in APG TBLs are reported here, and shed light on the complex phenomena present in these flows of great scientific and technological importance.

DOI: 10.1103/PhysRevFluids.8.L022602

Turbulent boundary layers (TBLs) play an essential role in a wide range of areas, including atmospheric flows, aircraft design, or turbine blades. Assessing the effect of streamwise pressure gradients on TBLs is critical to completely understand these applications [1,2], and this is very challenging due to the complex effect of flow history on the local state of turbulence [3–5]. Here we study adverse-pressure-gradient (APG) effects on TBLs on statistically two-dimensional flows subjected to a nearly-constant APG magnitude leading to near-equilibrium conditions [6,7]. As shown by Townsend [8] and Mellor and Gibson [9], in near equilibrium the mean velocity defect is selfsimilar in the outer region; this condition is achieved when the freestream velocity is prescribed by a power law. The turbulent character of the flow is analyzed through the Reynolds decomposition [10] of the fluid variables into a mean flow (averaged in time and the homogeneous spanwise direction) and a fluctuating component. Through this statistical approach, the mean flow has been extensively studied and some universal laws have been established, such as the law of the wall [11], the defect law and loglaw [12], together with various approaches to account for different flow

Published by the American Physical Society under the terms of the Creative Commons Attribution 4.0 International license. Further distribution of this work must maintain attribution to the author(s) and the published article's title, journal citation, and DOI. Funded by Bibsam.

configurations [13]. One important tool for mathematical modeling of physical systems is scaling, which in the context of turbulent flows has been used for assessing the physics at higher Reynolds numbers [14], and also in combination with symmetry analyses [15]. The approach taken in this work is based on scaling different energetic regions of the boundary layer at high Reynolds numbers, and it can be useful for other multi-scale systems where there are different energy scales interacting with each other. In these cases, a marginal integration of the scales of various sizes can lead to understanding the relative relevance and sensitivity of the various scales.

In this study we assess the fluctuating components of APG TBLs, denoted by Reynolds stresses (RSs), where the streamwise normal component $\overline{u^2}$ is the most energetic. Note that $\overline{(\cdot)}$ denotes the average in time and the homogeneous spanwise direction.

In APG TBLs we deal mainly with two parameters: the Reynolds number and the APG magnitude, where the latter can also be a function of the streamwise position. Kitsios *et al.* [5,16] used an integral approach to selfsimilarity in order to obtain scaling factors for the Reynolds stresses, and compared the spectra of a ZPG and an APG. The integral scaling factor they used was the displacement thickness, which is defined as $\delta^* = \int_0^{\delta_{99}} (1 - U/U_e) dy$, where U is the mean streamwise velocity and U_e is the velocity at the edge of the boundary layer ($y = \delta_{99}$). Note that x, y, and z are the streamwise, wall-normal and spanwise coordinates, respectively. Following this RS scaling, Maciel *et al.* [2] and Sanmiguel Vila *et al.* [17] scaled the outer peaks of the RSs with δ^* and δ_{99} for several numerical and experimental databases with a large range of APG magnitudes. In these studies, it was found that the wall-normal location of the outer peak of the RSs scales with δ^*, making it a scaling independent of the Reynolds number and APG effects.

Note that Maciel *et al.* [2] reflected on the δ^* scaling of the wall-normal location of the outer peak, y_{OP}. Since δ^*/δ_{99} decays slowly to zero when the Reynolds number tends to infinity, this would imply that the outer peak approaches the wall, therefore δ^* would only scale y_{OP}, but not necessarily the size of the outer region.

Despite the different values for the wall-normal location of the outer peaks in the RSs for moderate and strong APGs documented in Ref. [5], the spectral outer peak for the ZPG and the strong-APG cases were shown to be at the same wall-normal location: $y \approx \delta^*$. In other studies where δ_{99} was used for scaling the outer region of the TBL [3,18], the outer-spectral-peak wavelength λ_z appears to scale better in both ZPG and APG with δ_{99} than with δ^*.

Based on the work by Pozuelo *et al.* [19], in APG TBLs the wall-normal location and magnitude of the near-wall peak, denoted here by y_{IP} and $\overline{u^2}_{\mathrm{IP}}$ respectively, were found to increase with Reynolds number and APG magnitude using inner scaling. In this scaling, the viscous length $\ell_\tau = \nu/u_\tau$ and the friction velocity u_τ are employed, where ν is the fluid kinematic viscosity and $u_\tau = \sqrt{\tau_w/\rho}$ (where τ_w is the wall-shear stress and ρ is the fluid density). The superscript "+" will be used to denote inner scaling. Regarding the outer peak, its wall-normal location y_{OP} was found to be approximately constant when scaled with either the displacement thickness δ^* or the boundary-layer thickness δ_{99}, since for a moderate APG δ^*/δ_{99} decreases slowly with the Reynolds number. With the former length scale, y_{OP}/δ^* appeared to be less influenced by the APG, obtaining an approximate value of 1.4, while using δ_{99}, the locations varied with APG magnitude.

Analyzing the RS using the spanwise spectra with different scaling factors, we will assess similarities and differences with respect to the ZPG and the scaling properties of the RS. This has important implications in the context of the fundamental structure of turbulence.

In this study we analyze two high-Reynolds-number databases of well-resolved LES of ZPG [20] and APG TBLs [19], focusing on the near-equilibrium region in the APG, i.e., for $Re_\tau > 1000$. Note that Re_τ is the friction Reynolds number based on the friction velocity u_τ, and can be written as $Re_\tau = \delta_{99}/\ell_\tau = \delta_{99}^+$. The colors and line styles used for the two databases are shown in Table I.

The spanwise power-spectral density of a Reynolds-stress component $\overline{u_i u_j}(y)$ is denoted as $\phi_{u_i u_j}(y, k_z)$, where k_z is the spanwise wavenumber. Note that the integral over all the scales is equal to the total RS. Using this property, we can use an integral to determine the marginal contribution of small or large scales to the total RS (marginal contribution of energy, MCE). This can be written

TABLE I. (Left) Colors used to denote the contour lines of the two TBL databases and (right) line styles used to denote the analyzed profiles at different friction Reynolds numbers in the two TBL cases.

PG	Color	Re_τ	Style
APG	or	1000	——
ZPG	or	1500	- - -
		2000	.....

as follows:

$$\mathrm{MCE} = \int_{k_{z,c}}^{\infty} \phi_{u_i u_j} \mathrm{d}k_z \Big/ \int_{0}^{\infty} \phi_{u_i u_j} \mathrm{d}k_z, \tag{1}$$

where $k_{z,c}$ is the cut-off wavenumber. The spectra will be analyzed through contours of the premultiplied power-spectral density $k_z\phi_{u_i u_j}$ and contours of the marginal contribution to the RS as a percentage. Instead of the wavenumbers k_z, the contours will be represented against the spanwise wavelength $\lambda_z = 2\pi/k_z$.

The premultiplied spanwise spectra of the streamwise RS $k_z\phi_{uu}(y, \lambda_z)$ for both the APG and ZPG clearly show the near-wall and outer spectral peaks, as can be observed below in Fig. 2(a). The location of these spectral peaks can be scaled with a length scale to collapse the wall-normal position, here denoted as $y_{s\mathrm{IP}}$ and $y_{s\mathrm{OP}}$, and another length scale can be used to scale the wavelength of the peaks $\lambda_{z,s\mathrm{IP}}$ and $\lambda_{z,s\mathrm{OP}}$. In previous studies, the same scaling factor was used for the wall-normal location and for the wavelength λ_z; the novelty here is that we allow for a mixed scaling, i.e., the spanwise structures can have a different scaling than the wall-normal position where they are located, and Fig. 2(b) shows the success of this approach. A more complex analysis would be to determine the scalings for the energetic contours, since an energy scaling would be required for $k_z\phi_{uu}$, and the contours can be taken at a certain energy level or at a certain percentage of the peak or the maxima. For this last analysis the use of the MCE is useful.

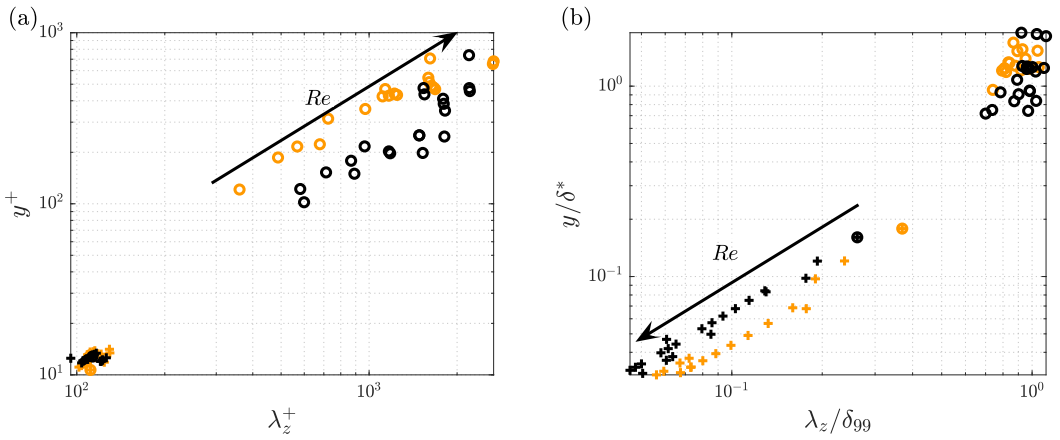


FIG. 1. Representation of the peaks in the premultiplied streamwise power-spectral density $k_z\phi_{uu}$ in (a) inner scaling and (b) scaling with boundary-layer and displacement thicknesses. Crosses denote the inner peak (IP) and circles for the outer peak (OP). Note that in (a) the inner peaks collapse by scaling the wall-normal position y and the wavelength λ_z in viscous units, and in (b) the outer peaks collapse when scaling y and λ_z with δ^* and δ_{99}, respectively. The black arrows show the direction of increasing Reynolds number.

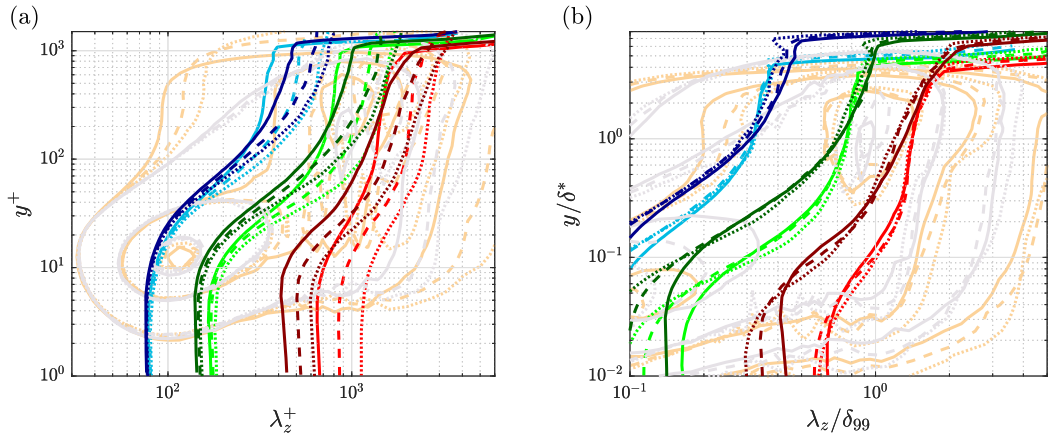


FIG. 2. Contours of the premultiplied spanwise power-spectral density of the streamwise RS, (a) scaled with the friction velocity, $k_z\phi_{uu}/u_\tau^2$, and (b) scaled with the edge velocity, $k_z\phi_{uu}/U_e^2$, both shown in lighter colors according to Table I. Contours taken at energy levels 0.5, 1.8, and 3.2 in panel (a). The levels for contours in panel (b) are: $[0.4, 1.2, 3] \times 10^{-3}$. The blue, green, and red lines represent the size of the scales where the accumulated energy from the smallest scales add up to 20, 50, and 80% of the total RS at that wall-normal location, respectively; for these lines, the light colors are used for the APG, while the dark colors are used for the ZPG.

The near-wall peak of $\overline{u^2}$ is closely connected with the spectral near-wall peak of $k_z\phi_{uu}$, thus it is natural to use the viscous scaling for this region, as shown in Fig. 1(a), for a number of profiles between $Re_\tau = 1000$ and 2000. This figure shows that the spectral inner peaks are located at approximately the same location for both APG and ZPG, at $y^+_{sIP} \simeq 12.5$, without a clear trend due to the resolution taken for the spectra close to the wall. The spanwise wavelenghts of the near-wall peak also collapse using inner scaling to a value $\lambda^+_{z,sIP} \approx 112$.

The outer peak of the RS is related with the spectral outer peak, and Fig. 1(b) shows that this spectral peak collapses in the premultiplied spectra. In particular, the wall-normal location of the outer peak scales with δ^* as in Ref. [5], while the spanwise wavelength λ_z scales with δ_{99} [3,18]. Again, due to the resolution of the spectral data, the values are slightly scattered. Our results show that the average y_{sOP}/δ^* is 1.3 for the APG and 1.1 for the ZPG. The average spanwise wavelenghts $\lambda_{z,sOP}/\delta_{99}$ are 0.91 for the APG and 0.96 for the ZPG. Considering the collapse of the inner and outer peaks in their respective scalings, then $y^+_{sIP}/\lambda^+_{z,sIP} = C_1$ and $(y_{sOP}/\delta^*)/(\lambda_{z,sOP}/\delta_{99}) = C_2$ are constant values. With the values above we obtain $C_1 \approx 0.1$ (for both ZPG and APG), and $C_2 \approx 1.43$ for APG and 1.15 for ZPG. Then the curves that the spectral outer peaks follow in Fig. 1(a) follow Eq. (2), and the spectral inner peaks in Fig. 1(b) follow Eq. (3). Note that $f(Re, \mathrm{PG}) = \delta^*/\delta_{99}$, where PG denotes the pressure-gradient magnitude,

$$y^+_{sOP} = \frac{y_{sOP}/\delta^*}{\lambda_{z,sOP}/\delta_{99}} \frac{\delta^*}{\delta_{99}} \lambda^+_{z,sOP} = C_2 f(Re, \mathrm{PG}) \lambda^+_{z,sOP}, \tag{2}$$

$$\frac{y_{sIP}}{\delta^*} = \frac{y^+_{sIP}}{\lambda^+_{z,sIP}} \frac{\delta_{99}}{\delta^*} \frac{\lambda_{z,sIP}}{\delta_{99}} = C_1 \frac{1}{f(Re, \mathrm{PG})} \frac{\lambda_{z,sIP}}{\delta_{99}}. \tag{3}$$

Since δ^* and δ_{99} are outer scales that can be measured in experiments [21], Eqs. (2) and (3) can be useful to estimate the location of the inner and outer spectral peaks in experiments where the spectra cannot be easily measured. Note that Eqs. (2) and (3) have been obtained with a simple manipulation of the scalings and the only argument needed to simplify the equation is the assumption that the inner and outer spectral peaks are fixed in their respective scalings. These equations can only be applied to APGs at high Reynolds numbers exhibiting separation of scales where the viscous scaling is valid,

i.e., it is not valid for large APG magnitudes where the flow is close to detachment and there is not an inner peak in the streamwise spectrum. Also note that our results for y_{OP} reported in Pozuelo *et al.* [19] are in agreement with Refs. [2,5,17], while $y_{s\mathrm{OP}}$ also scales with δ^* as in Kitsios *et al.* [5], in a case where the APG is at the verge of separation. The difficulties to distinguish trends using δ^* or δ_{99} arise from the fact that we have a mild APG, where δ^*/δ_{99} decreases very slowly with Reynolds number. For larger APG magnitudes, the decay of δ^*/δ_{99} is larger with Reynolds number, as can be observed when comparing the results for an APG at the verge of separation shown in Ref. [5] and the mild-APG in this work. The values for $y_{s\mathrm{OP}}/\delta^*$ are similar in both studies, confirming the δ^* scaling. As for the wavelength $\lambda_{z,s\mathrm{OP}}$, the scaling with δ_{99} leads to similar trends for the ZPG and the APG simulations as those documented in Refs. [3,18].

The magnitudes of the peaks are also relevant, since they indicate the energy scale that can be used to scale the energy contours of different regions. Pozuelo *et al.* [19] reported that $\overline{u^2}^+_{\mathrm{IP}}$ grows with Reynolds number and APG, however, we have observed that the values of the spectral near-wall peak appear to be constant with the Reynolds number and the value for the ZPG case is slightly higher ($\overline{u^2}^+_{s\mathrm{IP}} = 3.6$) than that of the APG case ($\overline{u^2}^+_{s\mathrm{IP}} = 3.4$).

Although the ZPG data does not exhibit an outer peak in the RS, the outer region scales with the edge scaling as well as the APG [19]; here we assess whether the spectral outer-peak magnitude scales using the square of the edge velocity U_e^2, which is determined in APG TBLs following the methodology described in Ref. [21]. Our results show that the variation of the values obtained in the outer peak of $k_z\phi_{uu}/U_e^2$ was too large to determine any trend, however, the average level is higher for the APG ($\simeq 4.5 \times 10^{-3}$) than for the ZPG case ($\simeq 3.4 \times 10^{-3}$).

In Fig. 2(a) we focus on the region around the spectral inner peak scaled in viscous units. It can be observed that the contours with $\lambda_z^+ < 400$, which are below $y^+ = 40$, scale properly in viscous units. The magnitude of the near-wall peak is lower for the APG, however, the energy around it is similar for the APG and the ZPG cases. The MCE blue contours representing 20% of the total $\overline{u^2}$ show that the smallest scales provide a similar contribution close to the wall at different Reynolds numbers and for both APG and ZPG. The 50 and 80% contours show the more prominent role of the large scales in this region with the APG, and also at higher Reynolds numbers. The green lines (MCE = 50%) below $y^+ = 10$ at $\lambda_z^+ \approx 140$ for the ZPG and $\lambda_z^+ \approx 170$ for the APG, are located in a region where the APG and ZPG have similar energy levels. The spectral inner peak is located between the blue and green lines, implying that these scales around the innerpeak add up to 30% of the energy. The light green lines are at a larger λ_z^+, showing that the APG spectral inner peak is slightly less energetic than in the ZPG case. The fact that $\overline{u^2}^+_{\mathrm{IP}}$ is larger at higher Reynolds numbers is explained by the impact of the wider scales (larger λ_z), which exhibit good scaling with δ_{99} as it can be seen in Fig. 2(b). The red lines indicate that the large scales contributing up to 20% of the total RS collapse for different Reynolds numbers all across the TBL and the APG largest scales are more energetic than those for the ZPG case.

In the outer region of the APG TBL it is also possible to differentiate two regions, the first one containing small energetic scales and another region of large scales surrounding the spectral outer peak. As observed in Fig. 1(b), using y/δ^* and λ_z/δ_{99}, the premultiplied spectral outer peak collapses for both APG and ZPG at different Reynolds numbers, although the value of the spectral outer peak is higher in the APG than for the ZPG case. Since the outer scaling with U_e^2 yields a good collapse of $\overline{u^2}$ in the outer region for both cases [19], the premultiplied spectra will be scaled with U_e^2, and the contours will be taken at a similar energy level.

In Fig. 2(b), the outer spectral peak at different Reynolds numbers are located around the same location for both APG and ZPG and its scales are of a similar size, however, the APG energizes the scales around that peak. The large scales above $y = \delta^*$ contribute in a similar proportion to the RS (up to their respective δ_{99}/δ^* values), independently of the Reynolds number or the APG (see red and green lines), while some differences start to be observed for the smaller scales (blue lines), since the APG contains more energy in smaller scales in this region. Between $y = 0.1\delta^*$ and $y = \delta^*$,

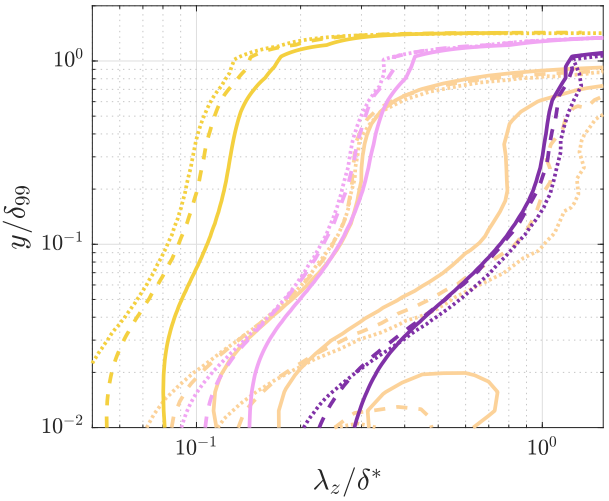


FIG. 3. Outer-scaled premultiplied power-spectral density of the streamwise RS, $k_z\phi_{uu}/U_e^2$. Contours taken at $[0.4, 1.2, 3] \times 10^{-3}$. The yellow, pink, and purple lines are the MCE contours at 0.1, 2.2, and 15%, respectively.

the large scales contribute in a similar way at different Reynolds numbers, but the relevance of the large scales is greater in the APG than in the ZPG.

In Fig. 3 we focus on the energetic small scales in the outer region of the APG. The energetic contours of $k_z\phi_{uu}/U_e^2$ are taken at the same levels as those in Fig. 2(b). The smaller energy level (light orange lines) collapses for scales of size $\lambda_z \approx 0.3\delta^*$ where the MCE is 2.2% (pink lines). Less energetic contours were investigated to assess whether the scaling λ_z/δ^* is still valid for smaller scales. This resulted in a behavior similar to what the yellow MCE contours show. Other scalings such as δ_{99} lead to further distancing of the energy contours for scales $\lambda_z < 0.3\delta^*$.

From the MCE contours it can be observed that the smallest scales in the outer region add up to 2.2% below $\lambda_z = 0.3\delta^*$ and 15% for scales $\lambda_z < \delta^*$. Although the energy contour levels around $\lambda_z = \delta^*$ do not exhibit any collapse with the Reynolds number, the MCE purple lines do, implying that the scales between $\lambda_z = 0.3\delta^*$ and $\lambda_z = \delta^*$ (pink and purple lines) contribute in a similar way to the total RS. The lack of collapse in the energy contours of the premultiplied spectra would in principle indicate that there is no similarity between the scales in this region; however, the MCE reveals that their marginal contribution is in fact very similar.

This small-scale energy in the outer region is not present in the ZPG, and the MCE contours do not exhibit any collapse, thus we did not include those contours in Fig. 3. The Reynolds shear stress was also analyzed. Its spectra in the near-wall region also scales in viscous units and even exhibits an inner peak in both APG and ZPG located at $y^+ \simeq 25$ and $\lambda_z^+ \simeq 105$. The energy level is similar in APG and ZPG using u_τ^2. The Reynolds shear-stress spectrum also develops an outer spectral peak in both APG and ZPG, which is centered around $y/\delta^* = 1.4$ and $\lambda_z/\delta_{99} = 0.9$. The energy of the outer spectral peak in the APG is almost twice the energy contained in its inner peak, while in the ZPG the values of the energy in its inner and outer peaks is similar.

The analysis of the $\overline{u^2}$ spectrum for APG TBLs conducted here included using different length scales for the wall-normal location and the spanwise wavelength. The inner region in TBLs with moderate APG exhibits the classical results reported for other wall-bounded flows, where the viscous scaling leads to marginal variations with Reynolds numbers. The wall-normal location of the outer spectral peak has been shown to scale with δ^* and its wavelength scales with a different outer scale: δ_{99}. While the MCE contours are also useful to observe the limits of the inner and outer scalings, they also reveal that the small-scale energy present in the outer region of APG TBLs scales with δ^*. The scales between $\lambda_z = 0.3\delta^*$ and $\lambda_z = \delta^*$ may have larger energy levels at higher

Reynolds numbers, but their MCE shows that they contribute in a similar proportion to the total outer energy level.

R.V. acknowledges the financial support provided by the Swedish Research Council (VR). P.S. and Q.L. were supported by the KAW Foundation. The computations and data handling were enabled by resources provided by the Swedish National Infrastructure for Computing (SNIC), partially funded by the Swedish Research Council.

[1] Z. Harun, J. P. Monty, R. Mathis, and I. Marusic, Pressure gradient effects on the large-scale structure of turbulent boundary layers, J. Fluid Mech. **715**, 477 (2013).
[2] Y. Maciel, T. Wei, A. G. Gungor, and M. P. Simens, Outer scales and parameters of adverse-pressure-gradient turbulent boundary layers, J. Fluid Mech. **844**, 5 (2018).
[3] A. Bobke, R. Vinuesa, R. Örlü, and P. Schlatter, History effects and near equilibrium in adverse-pressure-gradient turbulent boundary layers, J. Fluid Mech. **820**, 667 (2017).
[4] A. Tanarro, R. Vinuesa, and P. Schlatter, Effect of adverse pressure gradients on turbulent wing boundary layers, J. Fluid Mech. **883**, A8 (2020).
[5] V. Kitsios, A. Sekimoto, C. Atkinson, J. A. Sillero, G. Borrell, A. G. Gungor, J. Jiménez, and J. Soria, Direct numerical simulation of a self-similar adverse pressure gradient turbulent boundary layer at the verge of separation, J. Fluid Mech. **829**, 392 (2017).
[6] I. Marusic, B. J. McKeon, P. A. Monkewitz, H. M. Nagib, A. J. Smits, and K. R. Sreenivasan, Wall-bounded turbulent flows at high Reynolds numbers: Recent advances and key issues, Phys. Fluids **22**, 065103 (2010).
[7] H. M. Nagib and K. A. Chauhan, Variations of von Kármán coefficient in canonical flows, Phys. Fluids **20**, 101518 (2008).
[8] A. A. Townsend, *The Structure of Turbulent Shear Flow.* 2nd Edition (Cambridge University Press, 1976).
[9] G. L. Mellor and D. M. Gibson, Equilibrium turbulent boundary layers, J. Fluid Mech. **24**, 225 (1966).
[10] O. Reynolds, On the dynamical theory of incompressible viscous fluids and the determination of the criterion, Phil. Trans. R. Soc. A **186**, 123 (1895).
[11] T. Von Kármán, *Mechanical Similitude and Turbulence*, 611 (National Advisory Committee for Aeronautics, 1931).
[12] C. B. Millikan, A critical discussion of turbulent flow in channels and circular tubes, in *Proceedings of the 5th International Congress on Applied Mechanics*, Cambridge, MA 1938 (Wiley, 1939), pp. 386–392.
[13] P. Luchini, Universality of the Turbulent Velocity Profile, Phys. Rev. Lett. **118**, 224501 (2017).
[14] M. Hultmark, M. Vallikivi, S. C. C. Bailey, and A. J. Smits, Turbulent Pipe Flow at Extreme Reynolds Numbers, Phys. Rev. Lett. **108**, 094501 (2012).
[15] M. Oberlack, S. Hoyas, S. V. Kraheberger, F. Alcántara-Ávila, and J. Laux, Turbulence Statistics of Arbitrary Moments of Wall-Bounded Shear Flows: A Symmetry Approach, Phys. Rev. Lett. **128**, 024502 (2022).
[16] V. Kitsios, C. Atkinson, J. Sillero, G. Borrell, A. Gungor, J. Jiménez, and J. Soria, Direct numerical simulation of a self-similar adverse pressure gradient turbulent boundary layer, Int. J. Heat Fluid Flow **61**, 129 (2016).
[17] C. Sanmiguel Vila, R. Vinuesa, S. Discetti, A. Ianiro, P. Schlatter, and R. Örlü, Separating adverse-pressure-gradient and Reynolds-number effects in turbulent boundary layers, Phys. Rev. Fluids **5**, 064609 (2020).
[18] J. H. Lee, Large-scale motions in turbulent boundary layers subjected to adverse pressure gradients, J. Fluid Mech. **810**, 323 (2017).
[19] R. Pozuelo, Q. Li, P. Schlatter, and R. Vinuesa, An adverse-pressure-gradient turbulent boundary layer with nearly constant $\beta \simeq 1.4$ up to $Re_\theta \simeq 8700$, J. Fluid Mech. **939**, A34 (2022).

[20] G. Eitel-Amor, R. Örlü, and P. Schlatter, Simulation and validation of a spatially evolving turbulent boundary layer up to $Re_\theta = 8300$, Int. J. Heat Fluid Flow **47**, 57 (2014).

[21] R. Vinuesa, A. Bobke, R. Örlü, and P. Schlatter, On determining characteristic length scales in pressure-gradient turbulent boundary layers, Phys. Fluids **28**, 055101 (2016).